sustainability

MDPI

Article

Driving Safety and Comfort Enhancement in Urban Underground Interchanges via Driving Simulation and Machine Learning

Qian Liu [1], Zhen Liu [2,*], Bingyan Cui [3,*] and Chuanhui Zhu [1]

[1] The College of Electrical Engineering, Zhejiang University of Water Resources and Electric Power, Hangzhou 310018, China; zhchh@zjweu.edu.cn (C.Z.)
[2] School of Transportation, Southeast University, Nanjing 211189, China
[3] Department of Civil and Environmental Engineering, Rutgers, The State University of New Jersey, Piscataway, NJ 08854, USA
* Correspondence: zhenl_96@seu.edu.cn (Z.L.); bingyan.cui@rutgers.edu (B.C.)

Abstract: Urban transportation systems, particularly underground interchanges, present significant challenges for sustainable and resilient urban design due to their complex road geometries and dense traffic signage. These challenges are further compounded by the interaction of diverse road users, which heightens the risk of accidents. To enhance both safety and sustainability, this study integrates advanced driving simulation techniques with machine learning models to improve driving safety and comfort in underground interchanges. By utilizing a driving simulator and 3D modeling, real-world conditions were replicated to design key traffic safety features with an emphasis on sustainability and driver well-being. Critical safety parameters, including speed, acceleration, and pedal use, were analyzed alongside comfort metrics such as lateral acceleration and steering torque. The LightGBM machine learning model was used to classify safety and comfort grades with an accuracy of 97.06%. An important ranking identified entrance signage and deceleration zones as having the greatest impact on safety and comfort, while basic road sections were less influential. These findings underscore the importance of considering visual cues, such as markings and wall color, in creating safer and more comfortable underground road systems. This study's methodology and results offer valuable insights for urban planners and engineers aiming to design transportation systems that are both safe and aligned with sustainable urban mobility objectives.

Keywords: driving behavior; underground interchange; driving simulator; machine learning; traffic safety evaluation

Citation: Liu, Q.; Liu, Z.; Cui, B.; Zhu, C. Driving Safety and Comfort Enhancement in Urban Underground Interchanges via Driving Simulation and Machine Learning. *Sustainability* **2024**, *16*, 9601. https://doi.org/10.3390/su16219601

Academic Editors: Cristina Esteban, Francisco Alonso and Mireia Faus

Received: 1 October 2024
Revised: 29 October 2024
Accepted: 1 November 2024
Published: 4 November 2024

1. Introduction

With the accelerating process of urbanization and the sharp rise in the number of motor vehicles, the construction of urban interchanges, particularly underground interchanges [1,2], has progressed swiftly. Underground interchanges, with their advantages of effectively alleviating ground traffic pressure and improving traffic efficiency, have gradually become an important means of solving urban traffic congestion problems [3,4]. However, the unique environment of underground interchanges has a significant impact on drivers' vision, psychology, and driving behavior, which in turn affects driving safety and comfort [5,6]. Ensuring driving safety in these environments is also crucial for achieving urban sustainability, as safe and efficient transportation systems reduce accident-related delays and emissions [7,8]. Therefore, studying how to improve the driving safety and comfort of underground interchanges has become an important topic in the current field of urban infrastructures.

In recent years, with the continuous increase in urban traffic pressure, underground interchanges, as one of the important means to alleviate traffic congestion, have garnered

widespread attention regarding their driving safety and comfort issues [9]. Many scholars have conducted extensive research in this field [10–12], mainly focusing on the setting of traffic signs and markings [13,14], driving simulation [15,16], road safety evaluation [17,18], and driving behaviors [19,20].

(1) The setting of traffic signs and markings: underground interchange spaces are enclosed, and the environment is relatively monotonous, with driving being significantly affected by the side walls [21]. For systematic multi-point entry and exit underground roads in particular, a signage system is needed to guide exits; due to the special environment of underground interchanges, drivers have a strong reliance on signs, making the setting of traffic signs more demanding than above ground. Hsu et al. studied the setting of traffic signs and markings in underground interchanges, optimizing the placement positions and spacing of signs based on drivers' reaction time and visual recognition distance [22]. Zhang et al. examined and optimized the visibility of underground roads through analytical methods, emphasizing the importance of properly setting signs to enhance driving safety [23]. These studies, through theoretical deduction methods, proposed critical strategies for the proper placement of signs in underground interchanges to enhance driving safety.

(2) Driving simulation: driving simulators have extensive applications in the field of road research [24]. Driving simulators can obtain traffic operating characteristics of drivers under various road and traffic conditions [25], such as speed, acceleration, lane deviation, and steering wheel angle, offering robust support for driving behavior analysis with comprehensive data. Sun et al. studied car-following and lane-changing behaviors in the diverging areas of tunnel-interchange connection segments using a driving simulator [26]. The study explored the effects of road characteristics, sign information volume, and traffic conditions on driver behavior, analyzing the driving performance of 25 participants in 72 simulated road models, and found that connection distance and sign information volume significantly affect driving behavior. Liu et al. employed driving simulation and data mining methods to investigate the impact of safety facilities in underground interchanges on driving safety and comfort [27]. The research found that properly shortening the length of deceleration segments, installing reasonable warning signs at merging points, and adjusting wall colors can significantly enhance driving safety and comfort. However, the data processing in these studies is relatively complex, and automated evaluation of driving safety has not been realized.

(3) Road safety evaluation: underground interchange spaces are enclosed, and the environment is relatively monotonous, with driving being significantly affected by the side walls [28]. He et al. found that optimized tunnel wall luminance and uniform lighting conditions improve driver visual stability and reduce visual load, enhancing driving safety in highway tunnels [29]. Yeung and Wong, through analyzing traffic accident data of urban underground roads, found that the accident rate at tunnel entrances is the highest, indicating that optimizing tunnel entrance design and improving driver attention are crucial for reducing accidents [30]. Su et al. improved traffic safety by optimizing the light environment in highway tunnels [31]. This study systematically considered multiple influencing factors, optimized tunnel lighting quality, and improved drivers' visual performance, thereby elevating the driving safety level in tunnel areas. Unfortunately, there is currently a lack of clear evaluation criteria for driving safety and comfort in underground interchanges.

(4) Driving behaviors: when driving in an underground interchange environment, drivers' physiological and psychological states are influenced by the surrounding environment, leading to fluctuations [32]. Szydłowski et al. investigated drivers' psychomotor reaction times and developed a standardized testing method to assess drivers' reaction times to various external stimuli [33]. The research found that reaction time is a crucial factor influencing driving safety; proper road design and driver assistance systems can significantly enhance driving safety. These physiological and psychological fluctuations can impact drivers' ability to perceive information from the surrounding environment, thereby affecting their driving behavior and easily causing them to make incorrect decisions.

In summary, significant progress has been made in research on the safety and comfort of driving on underground roads both domestically and internationally, but there are still some urgent issues to be addressed. Firstly, the standards for traffic signs and marking placement need to be further refined to suit the complex underground road environment. Secondly, there is no clear process and method for safety evaluation based on driving simulators, and the standardization and scientific nature of driving simulation tests also need to be further studied. In addition, data processing and evaluation methods lack advanced technical means. Research on risk assessment and early warning systems based on driving behavior needs to be strengthened to enhance drivers' safety awareness and reaction capabilities. This study will integrate the research findings and utilize driving simulation and machine learning methods to systematically analyze the impact of underground road environments on driving safety and comfort, thereby providing a scientific foundation for the planning and design of underground roads.

This study has the following three contributions:

(1) Developed an evaluation model for driving safety and comfort in underground roads based on driving simulation experiments.
(2) Investigated the combined effects of various traffic signs and markings, tunnel wall colors, and speed bump lengths on driving behavior.
(3) Utilized machine learning methods to classify and predict driving safety and comfort, offering a scientific foundation.

The rest of this paper is organized as follows: Section 2 describes BIM modeling driving simulation and machine learning methods; Section 3 discusses experimental details, prediction results, and findings; finally, Section 4 concludes this study.

2. Methodology

2.1. Modeling and Transformation

The construction of the underground interchange two-dimensional CAD graphics is the basis of the 3D model. As shown in Figure 1, firstly, the modeling target road section was determined according to the original design data of the underground interchange and combined with the aerial photography results. The 2D plan of the underground interchange was drawn in AutoCAD, and the size of each area unit was calibrated, followed by 3D modeling.

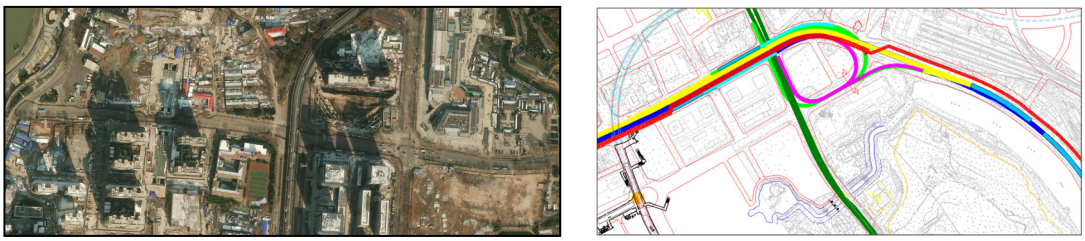

(**a**) Aerial map (**b**) AutoCAD map

Figure 1. Flow chart for analysis of meteorological conditions and characteristics.

To transform the 2D CAD underground interchange graphics into a high-precision BIM 3D model, the operation needed to be performed in 3ds Max. First, the established 2D CAD underground interchange DWG drawing was opened in 3ds Max, and the line type was added as a new project line-type pattern. After modeling, textures and materials needed to be added to the model. The material editor in 3ds Max was used to adjust the color, brightness, reflectivity, and other properties of materials and textures to make the buildings more realistic. Real road wall photos were used for mapping, as shown in Figure 2, making the model appear closer to the actual road in the driving simulator.

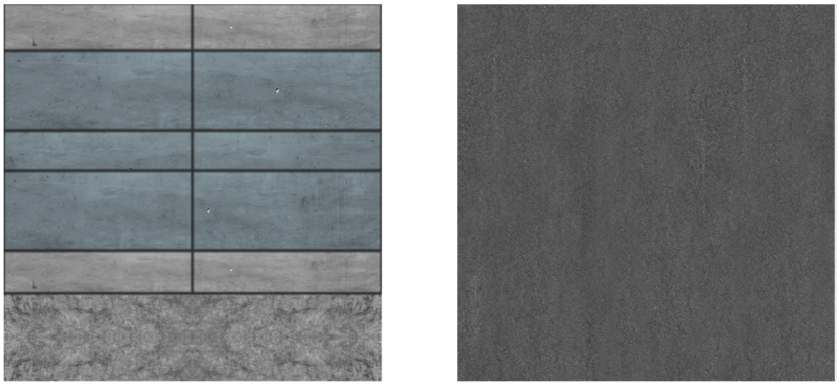

(**a**) Regional division (**b**) Concrete material

Figure 2. Texture map of the model.

After creating the model, the scene was rendered using the 3ds Max renderer. The renderer's settings were adjusted, including ray tracing depth, reflection, refraction, and other parameters to obtain more realistic effects. Afterward, the model needed to be imported into the SCANeR STUDIO platform for driving simulation. SCANeR STUDIO was used as the control software, providing five main modules to restore tunnel details, as shown in Figure 3.

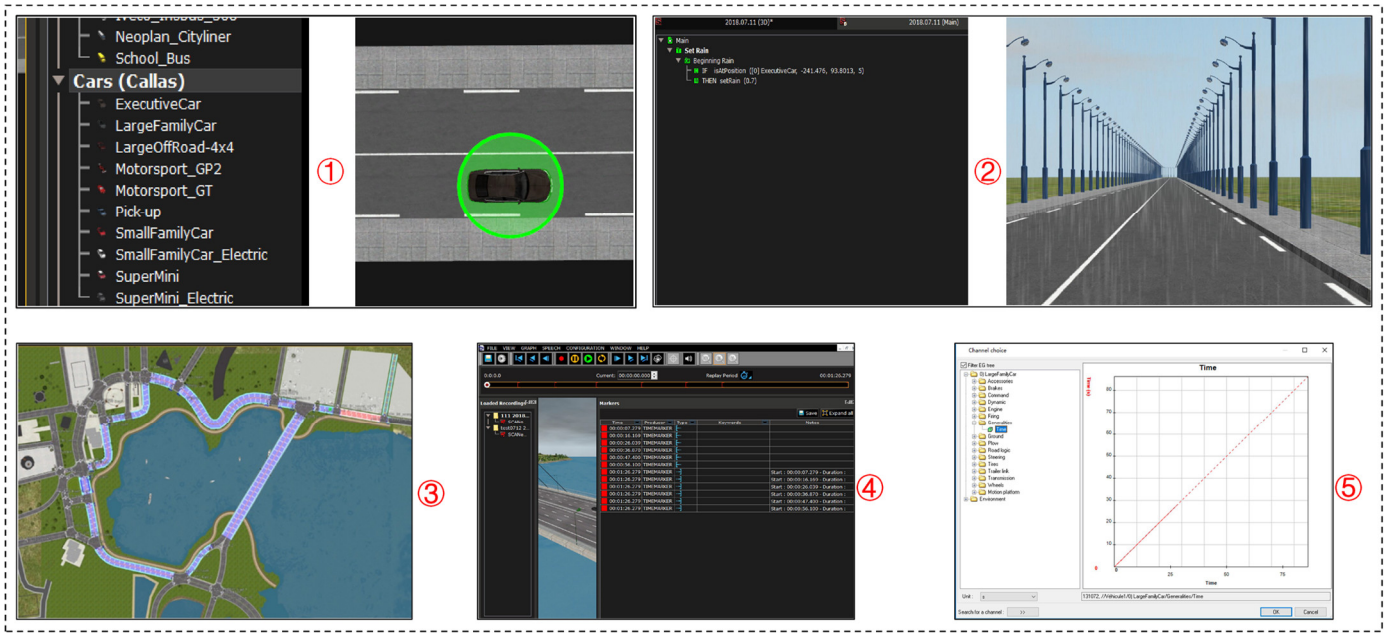

Figure 3. Five functional modules in the SCANeR STUDIO software.

(1) Vehicle module: this module was used to create a mathematical model of the test vehicle, simulating realistic vehicle dynamics and response. The vehicle's specifications, such as acceleration, braking, and handling characteristics, were configured to match the typical performance of vehicles commonly used in underground interchanges.

(2) Terrain module. in this module, we designed the road networks with all necessary logical information, including signage, traffic lights, and speed limits, to recreate realistic underground interchange scenarios. This setup allowed us to test driver reactions to common features within underground interchanges, such as entry and exit signs and deceleration zones.

(3) Scene module: this module was essential in constructing a detailed 3D model of the tunnel environment, including vehicles, terrain, and road infrastructure. By creating an

immersive scene, we could simulate a realistic underground interchange to evaluate driver responses in a controlled yet realistic environment.

(4) Analog module: we used this module to control and monitor the entire simulation process, managing the synchronization of the simulation's elements and ensuring that the test conditions were consistent across participants. The analog module helped us systematically manage the tests and ensure repeatability of the simulation environment.

(5) Analysis module: this module was utilized to process and analyze the data collected during the simulation. Key parameters, such as vehicle speed, acceleration, lateral offset, and steering angle, were extracted to assess driving safety and comfort. Additionally, this module allowed us to visualize the results using 3D animations and data tables, supporting a detailed analysis of driver behavior in response to various scenarios.

2.2. Driving Simulator Scheme

2.2.1. Working Condition Design

The driver needs to decelerate before entering the tunnel. To address this issue, longitudinal deceleration markings in the driving direction and entrance signs are set at the tunnel entrance to remind the driver. Additionally, prolonged driving in a tunnel can cause driver fatigue, leading to inattention and distraction, which increases the accident rate. Therefore, the choice of tunnel wall color is essential. Considering the impact of these factors on the driving safety of the underground interchange, four areas have been addressed: the entrance and exit, the approach road, the tunnel walls, and the diversion and confluence sections. Based on the existing traffic signs and markings, a basic scheme meeting the norms and preliminary traffic needs of the passageway was established to verify the impact of traffic signs and markings on driving. Nine optimization schemes were developed to improve different aspects, including the color of the tunnel wall, entrance deceleration lines and signboards, exit warning boards, and two merge warning boards, as shown in Table 1.

Table 1. Summary of working conditions.

Scheme Number	Details
1 #	Default scheme (The walls are white, blue and white, and the top is black)
2 #	The wall color is white at the top, and the wall is white blue white
3 #	The wall color is black at the top and white blue at the wall
4 #	Speed bump type is landscape (default is portrait)
5 #	Length of speed bump is 80 m (default is 60 m)
6 #	Length of speed bump is 40 m (default is 60 m)
7 #	The entrance signs are marked in Chinese pinyin
8 #	Add a sign 250 m from the exit
9 #	Add road information at the diversion 1
10 #	Add a side arrival reminder at confluence 2

2.2.2. Simulation Process

Using the 3ds Max and SCANeR software platforms, an immersive simulated driving environment was researched and built according to the above-mentioned underground interchange design scheme and combined with on-site research. This environment had a high degree of restoration and perfect, adjustable working parameters. A total of 24 volunteers participated in the experiment voluntarily, with 80% of the subjects being men and 20% being women, reflecting the statistical characteristics of Chinese drivers.

The driving simulator was set to record vehicle operating parameters at a frequency of 20 Hz, including speed, acceleration, lateral offset, accelerator, brake, steering wheel angle, clutch, and vehicle coordinates. This frequency was more conducive to capturing changes in drivers' driving behavior details and obtaining richer experimental data.

Before the official experiment started, there were about 5 min of driving practice. During the formal experiment, each person conducted ten groups of experiments in a

random order, with each scene lasting about 3 min. The prepared tunnel model was imported into the simulator, and once ready, the experimenter entered the cockpit to start the simulation test. The starting point of the test was far enough from the tunnel entrance to allow driving through the tunnel at a speed of less than 60 km/h.

The set-up scene in SCANeR STUDIO is shown in Figure 4. After completing the driving simulation, the file location can be selected, and the data can be exported for further analysis. The final specific design parameters of the underground interchange model are as follows: the total length of the model is 2.5 km, the speed limit is 60 to 80 km/h, the model has six two-way lanes (each lane width is 3.75 m), and the net boundary height of the building is 5 m.

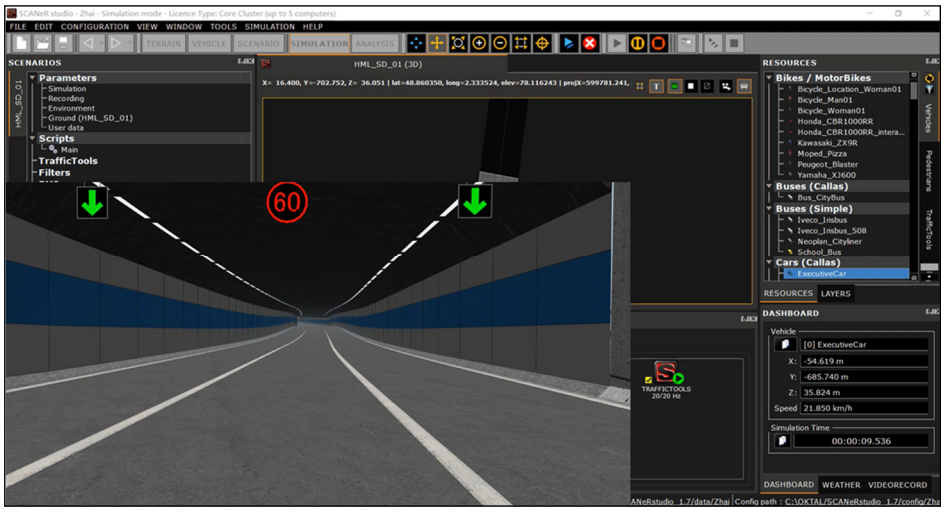

Figure 4. Driving simulation model of underground interchange in SCANeR STUDIO.

2.2.3. Evaluation Index

(1) Driving Behavior and Its Indicators

Driving behavior is a multi-dimensional concept, encompassing both longitudinal and lateral parameters. Longitudinal and lateral parameters were derived from the vehicle's speed and position data, measuring control over speed (acceleration and deceleration) and lateral positioning within the lane. For instance, steering wheel torque data were used to assess the driver's steering response, while lateral acceleration was calculated to evaluate stability during maneuvers.

(2) Safety indicators

The index evaluation mainly revolves around the driving performance of the car. This traditional method primarily regards the car as a mass point or a rigid body and uses driving speed to evaluate driving safety. The first approach is based on the evaluation standard of vehicle speed, where design quality is judged according to the range of the difference between the design speed and the operating speed. The second approach evaluates the size of the acceleration, considering both acceleration and deceleration scenarios. Additionally, the accelerator pedal is a crucial means for the driver to control the vehicle's power system. Its position, depth, and usage have a significant impact on driving safety and should be included in the safety control index.

(3) Comfort indicators

To evaluate driving comfort, lateral acceleration is a vital evaluation index. Acceleration disturbance is defined as the standard deviation of vehicle acceleration from the

mean acceleration, as shown in Equation (1). It reflects the degree of change in vehicle acceleration, indicating the fluctuation of acceleration during vehicle operation.

$$\sigma = \sqrt{\frac{\int_0^T \left[(a(t) - \overline{a})^2 \right] dt}{T}} \quad (1)$$

where σ represents the disturbing acceleration (m/s^2); T denotes the total observation time (s); $a(t)$ denotes the acceleration at time t (m/s^2); $\overline{\alpha}$ represent the average acceleration (m/s^2).

Steering wheel torque is an important index for measuring driving comfort. It refers to the torque required to manipulate the steering wheel and is also one of the direct tactile sensations between the driver and the vehicle. When the actual characteristic or expected characteristic is a continuous curve, the average value of the function $L(y)$ in a specific interval [a, b] is taken as the comfort loss of the steering wheel torque characteristic in this interval, as shown in Equation (2) where l is the comfort loss; k is the loss factor; $y(x)$ and $m(x)$ are the steering wheel torque properties preferred by the driver and actually provided by the vehicle, respectively.

$$l = \frac{1}{b-a} \int_a^b k[y(x) - m(x)]^2 \, dx \quad (2)$$

2.2.4. Data Preprocessing

The vehicle driving behavior data were exported through the analysis module of the SCANeR STUDIO software (version 2021), which included speed, acceleration, lateral offset, accelerator, brake, steering wheel angle, clutch, vehicle coordinates, and other parameters. Initially, the experimental data were collected in an irregularly sorted TXT format and could not be processed directly. Before data processing, the data needed to be preliminarily organized and imported into Excel for classification. Subsequent analysis operations could only be carried out after orderly sorting, as shown in Table 2.

Table 2. Parameters, values and their description.

Index	Data Type	Details
(X, Y)	Position coordinates	To determine the driver's position in the model
Distance from key point	Position coordinates	To describe the driver's distance from the key point, which is positive when not reached and negative after passing (m)
Steering wheel torque	Comfort indicator	The torque applied to the steering wheel per unit time (N·m)
Lateral acceleration	Comfort indicator	Lateral acceleration applied to the vehicle (m/s^2)
acceleration	Safety indicator	The acceleration of the vehicle in the driving direction (m/s^2)
Disturbing acceleration	Comfort indicator	The size of the velocity swing (m/s^2)
Velocity	Safety indicator	The speed of the vehicle in the driving direction (m/s)
Gas pedal	Safety indicator	To describe throttle efficiency with a minimum value of 0 and a maximum value of 1 (%·s)

2.3. Machine Learning Analysis

Gradient Boosting Decision Tree (GBDT) is a commonly used machine learning classification model. Its basic idea is to use weak classifiers (decision trees) to obtain the optimal model for iterative training [34,35]. GBDT has the advantage of a good training effect and is not easy to over fit. LightGBM has been improved on its basis so that it has faster training speed, lower space consumption, higher accuracy, and XGBoost (eXtreme Gradient Boosting) for the weakness and overfitting problems when dealing with extensive data. The

problems mentioned above are solved by LightGBM adopting the distributed processing method. Its core modules are as follows.

2.3.1. Histogram-Based Decision Tree

In the traditional decision tree algorithm, each time the optimal feature was selected for splitting, all the features needed to be sorted, and each feature's information gain or Gini index was calculated [36]. The problem with this approach is that when the number of features is large, the computation can be extensive, resulting in a long training time. LightGBM uses the histogram algorithm to solve this problem. The basic idea is to discretize the continuous floating-point eigenvalues k into integers and simultaneously construct a histogram with a width of k. As the data are traversed, statistics are accumulated in the histogram based on the discretized value as an index. After traversing the data once, the histogram accumulates the required statistics [37]. Then, it traverses the histogram to find the optimal segmentation point according to the discrete values, as shown in Figure 5. After the features are discretized, the two most direct benefits are reduced memory usage and lower computing costs, which lay the foundation for LightGBM to handle big data efficiently.

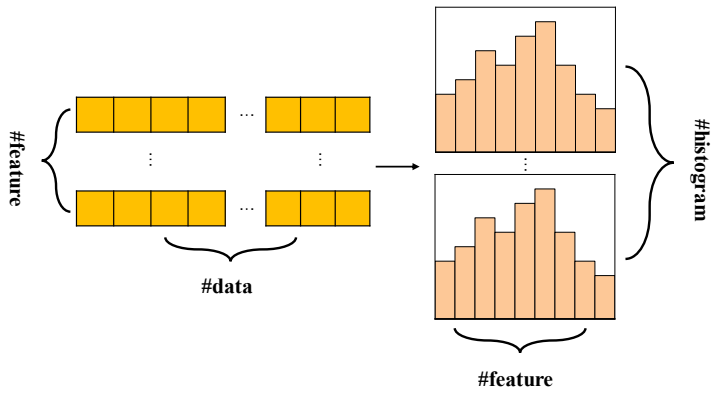

Figure 5. Histogram-based decision tree of LightGBM.

On the other hand, LightGBM has also improved the original histogram algorithm to optimize the running speed. Specifically, LightGBM-adopted difference acceleration. The histogram of a leaf node can be obtained by the difference between the histogram of its parent node and the histogram of its brother. In the process of building the tree, LightGBM can also use the histogram to make differences to obtain the leaf node with a large histogram to obtain the histogram of its brother leaf at a minimal cost. These optimizations can make LightGBM more efficient and accurate when training large-scale data, as shown in Figure 6.

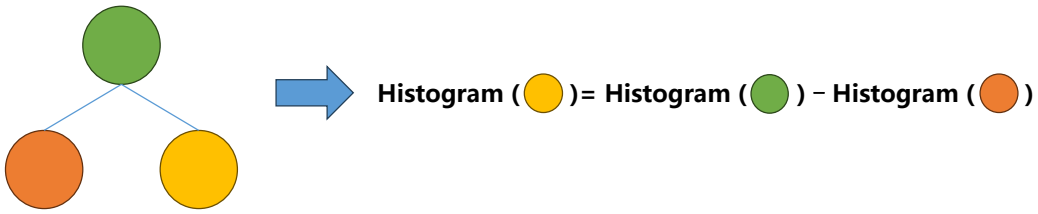

Figure 6. Subtraction and acceleration of histogram.

2.3.2. A Leaf-Wise Strategy with a Depth Limit

LightGBM has been further optimized based on the histogram algorithm. Compared with the level-wise decision tree growth strategy adopted by most GBDT tools, LightGBM adopts the leaf-wise growth algorithm with depth limitation. The algorithm can more efficiently search for the node with the maximum gain for splitting so that the depth of the tree is smaller, the model complexity is lower, and it is less likely to be overfitted.

LightGBM was selected over other models like XGBoost due to its unique advantages in handling large-scale data with high efficiency [38]. Unlike XGBoost, which employs a level-wise tree growth strategy, LightGBM's leaf-wise approach allows it to converge faster and achieve higher accuracy, particularly for datasets with numerous features. Additionally, LightGBM supports histogram-based decision tree methods, reducing memory usage and computational time. These advantages make LightGBM well-suited for our study, where processing large volumes of simulation data efficiently is essential.

As shown in Figure 7, compared with the traditional level-wise growth strategy, the leaf-wise strategy of LightGBM selects the leaf with the most significant splitting gain from all the current leaves for splitting, thus avoiding the waste of useless splitting. Compared with level-wise, leaf-wise can reduce errors and get better accuracy with the same number of splits, but it may lead to overfitting. Therefore, LightGBM adds a maximum depth limit to prevent overfitting and improve the model's accuracy while ensuring high efficiency.

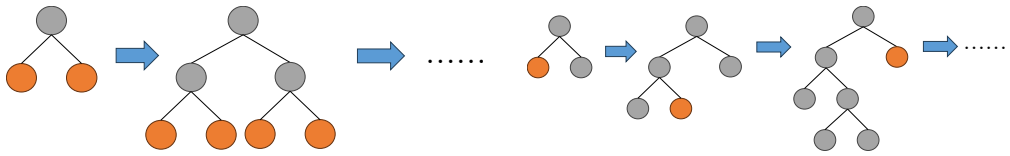

(**a**) Traditional layer by layer growth (**b**) Leaf growth

Figure 7. Decision tree.

2.3.3. Gradient-Based One-Side Sampling

Gradient-based One-Side Sampling (GOSS) algorithm, after adding the traditional GBDT algorithm, referred to as GOSS technology, can only retain extensive gradient data with a significant information gain when collecting data samples, thereby improving sampling efficiency. At the same time, to discard the influence of some data overall, GOSS adopts the means of expansion to compensate for the data with a slight gradient in the gain sorting.

Specifically, GOSS first sorts of the data according to the absolute value of the gradient, selects the first $a * 100\%$ data with the most considerable absolute value, and then randomly selects $b * 100\%$ data from the remaining data. Then, when calculating the information gain, the sampled small gradient data samples are multiplied by the constant $(1 - a)/b$, and the total data is still 100%. The algorithm pays more attention to under-trained instances and does not change the distribution of the original dataset too much.

2.3.4. Exclusive Feature Bundling

Finally, LightGBM uses the exclusive feature bundling EFB (Exclusive Feature Bundling) algorithm to reduce dimensionality when collecting data to improve the calculation speed. Specifically, bundling two features that are not mutually exclusive reduces the number of features without affecting the final accuracy, thereby reducing the time consumed by LightGBM when processing high-level, complex data sets. The conflict ratio is usually used to measure the degree to which two features are not mutually exclusive. When this value is small, the two features can be bundled.

2.3.5. Model Evaluation

To evaluate the driving safety and comfort evaluation model of the underground interchange based on LightGBM, it is necessary to use common evaluation indicators in machine learning classification tasks. The most common binary classification task is taken as an example. The results can be divided into four cases [38]: true positive (True Positive, TP), false positive (False Positive, FP), false negative (False Negative, FN), and true negative (True Negative, TN); they can be represented by a 2×2 order confusion matrix. There are two types of descriptions for the prediction results: one is the description of whether the prediction results are correct or not, the same as the actual results are true (True), and the difference is false (False); the other is the description of the prediction results

in themselves, where the results of a value of 1 is positive (Positive), and a result of 0 is negative (Negative) [39,40]. According to the different situations of the confusion matrix, the classification task also has several evaluation indicators to illustrate:

(1) Accuracy: accuracy indicates the proportion of correctly classified results to the total number of samples, i.e., the proportion of TP and TN in the matrix to the total samples, as shown in Equation (3).

$$Accuracy = \frac{TP + TN}{TP + TN + FP + FN} * 100\% \quad (3)$$

(2) Precision (Precision): the precision rate indicates the proportion of correct predictions in all samples with positive prediction results, also known as the precision rate, as shown in Equation (4).

$$Precision = \frac{TP}{TP + FP} * 100\% \quad (4)$$

(3) Recall rate (Recall): the recall rate indicates the proportion of correct predictions in all samples whose accurate results are positive, also known as the recall rate, as shown in Equation (5).

$$Recall\ rate = \frac{TP}{TP + FN} * 100\% \quad (5)$$

(4) F_1 score: due to the interaction between the precision rate and the recall rate, in order to comprehensively evaluate the two, the F1 value is generally used for reconciliation, as shown in Equation (6).

$$F_1 = \frac{2 * Precision * Recall}{Precision + Recall} * 100\% \quad (6)$$

(5) ROC curve and AUC value: the ROC curve is a curve drawn with the false positive rate (False Positive Rate) as the abscissa and the actual positive rate (True Positive Rate) as the ordinate, as shown in Equation (7). The AUC value is the area under the ROC curve used to measure the classifier's performance. The more significant the ROC value, the better the classification effect.

$$TRR = \frac{TP}{TP + FN} * 100\%,\ FPR = \frac{FP}{FP + TN} * 100\% \quad (7)$$

Compared with the P-R curve, the ROC curve is not sensitive to whether the samples are balanced, and its shape does not change significantly with the distribution of positive and negative samples. Therefore, the ROC curve is used here to evaluate the classification task.

2.4. Experimental Design

2.4.1. Experiment and Data

In the traditional decision tree algorithm, each time the optimal feature was selected for splitting, all the features needed to be sorted, and each feature's information gain or Gini index was calculated.

Model training and evaluation were completed in the Win10 system, configured with Intel (R) Core (TM) i5-9300H CPU @2.40GHz; the memory was 16 GB; and model code was compiled on Pycharm, Python version 3.8.

In view of LightGBM's features such as more efficient parallel training, faster processing of large amounts of data, and low memory consumption [41], this paper chooses to use it to establish a classification model of driving safety and comfort levels based on multi-factor indicators. A total of 12 independent variable indicators were selected, and the

evaluation grade fitted in the first section was taken as the output variable. The specific distribution of each variable is shown in Table 3. According to the sampling frequency set by this study, a total of 257,543 samples were generated from 240 sets of experimental data from 24 drivers (the age distribution between 18 and 45). Of these, 12,944 were in the entrance section, 15,675 were in fractional confluence Section 1, 14,386 were in fractional confluence Section 2, 12,404 were in the exit section, and the rest were in the basic section. Then, 80% of all samples were used as the training set and 20% as the test set.

Table 3. Input and output for machine learning models.

Type		Parameters	Variable Details	Number
Input	Driving behavior	α	Lateral (α_{La}) and Longitudinal (α_{Lo})	2
		S_{wt}	Steering wheel torque	1
	Traffic safety facilities	Speed bump	Length (Sb_L) and type (Sb_t)	2
		Sign	Entrance (S_{En}), exit (S_{Ex}), diverting (S_d), and confluence (S_c) sections	4
		Wall color	W_c	1
	Vehicle location	Time	t	1
		D	Distance from the Entrance (D_{En}), exit (D_{Ex}), diverting (D_d), and confluence (D_c) sections	1
Output	Safety and comfort	Evaluation grade	Low grade = 1, moderate grade = 2, high grade = 3	1

2.4.2. Model Parameters

After the database is built, the input parameters of the model need to be set. In LightGBM, there are several model parameters, including boosting, objective, num_class, seed, num_leaves, learning_rate, n_estimators, max_depth, and so on. Among these indexes, num_leaves, max_depth and learning_rate have a great influence on the final precision and accuracy of the model. To ensure the accuracy of the model and prevent overfitting, the recommended values of different combinations are set as follows:

(1) num_leaves: 5, 10, 15, 20, and 25;
(2) max_depth: 3, 4, 5, 6, and 7;
(3) learning_rate: 0.03, 0.05, 0.07, 0.1, and 0.12.

GridSearchCV module of the machine learning tool library scikit-learn was used for parameter traversal search to obtain the optimal parameter setting values.

3. Results and Discussion

3.1. Prediction Results of Driving Safety Level

3.1.1. Evaluation Results of Prediction Model

According to the input model parameters and database, the LightGBM machine learning model is used to classify and evaluate the driving simulation data of the entrance, diversion, confluence, exit, and basic sections. The indicators for evaluating driving safety and comfort levels are then output. Table 4 compares the results of the LightGBM model with those of other mainstream models, with the evaluation index being the average of the five sections. The classification results of the LightGBM model are significantly higher than those of other mainstream models, with each index value exceeding 90%. This is because this model allows it to handle complex patterns in the data more efficiently. Unlike traditional classifiers like Random Forest or Logistic Regression, which utilize a level-wise approach, LightGBM's leaf-wise method enables it to better capture high-dimensional interactions within the driving behavior data, resulting in faster convergence and improved accuracy.

Table 4. Evaluation results of four classification models.

Model	Accuracy	Presidion	Recall Rate	F_1 Score
LightGBM	97.2%	96.4%	92.9%	94.6%
WEIGHTEDClassifier	96.5%	92.5%	89.5%	90.8%
LRClassifier	91.5%	91.4%	87.5%	88.2%
RFClassifier	87.6%	85.8%	81.8%	83.5%

Furthermore, the classification results of the LightGBM model under the five sections are statistically analyzed. The results are shown in Figure 8, and the confusion matrix is shown in Figure 9. It is evident that LightGBM has strong classification performance across all indicators, with average accuracy, F_1 score, and precision reaching 97.06%, 94.5%, and 96.42%, respectively. Among them, LightGBM performs best in the classification task of the exit section, achieving the highest scores in all parameters. This may be due to the significant changes in driving safety and comfort in the exit section, specifically reflected in the greater impact of changes in traffic safety facilities and more noticeable changes in driving behavior data. This provides distinct data patterns for LightGBM to learn and classify effectively. Therefore, LightGBM can better capture these changes, resulting in better classification performance. In contrast, in the basic segment, there is a large amount of data with less noticeable changes in evaluation levels, and many features require attention, making it difficult to identify key quantities. The classification ability of LightGBM is more intuitively reflected in the ROC curve and AUC value, as shown in Figure 10.

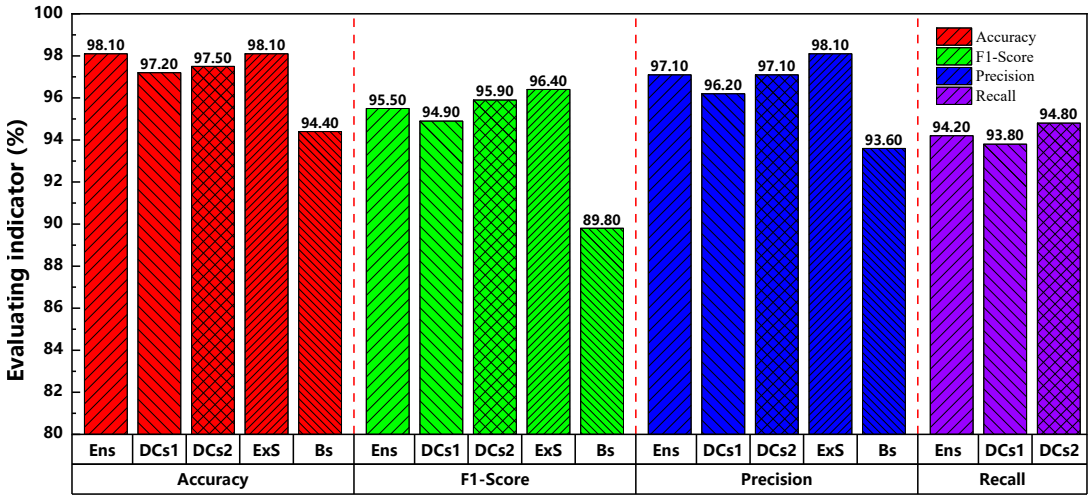

Figure 8. Output index values of different segments of LightGBM classification model.

3.1.2. Feature Importance Ranking

Reasonable index selection is vital for building a high-accuracy, high-precision model. To study the influence of each parameter on the model's performance, the model importance output function from the LightGBM library was used to analyze the 12 items of the dataset for the entrance and exit sections of the underground interchange, the dataset for the separation and confluence sections, and the dataset for the basic section. The importance of variable indicators was output and sorted, with the specific feature importance rankings shown in Figure 11. LightGBM model calculates importance based on the contribution of each feature to model accuracy. This is achieved by assessing the total gain of each feature, which represents how much the feature improves model prediction when used for a split in the decision tree. Features with higher total gains are ranked as more important, as they have a stronger influence on model predictions.

Predicted value / Ture value	1	3	2
1	98.84%	0.22%	0.94%
3	6.67%	85.33%	8.00%
2	1.46%	0.16%	98.39%

(**a**) Entrance section

Predicted value / Ture value	2	3	1
2	98.83%	0.08%	1.09%
3	6.76%	86.94%	6.31%
1	1.04%	0.09%	98.87%

(**b**) Diverting and confluence sections 1

Predicted value / Ture value	1	2	3
1	98.53%	1.34%	0.13%
2	1.59%	97.94%	0.47%
3	4.47%	7.67%	87.86%

(**c**) Diverting and confluence sections 2

Predicted value / Ture value	1	3	2
1	97.09%	0.35%	2.56%
3	6.96%	85.51%	7.54%
2	0.80%	0.49%	98.71%

(**d**) Exit section

Predicted value / Ture value	1	3	2
1	93.62%	0.42%	5.96%
3	14.16%	70.39%	15.45%
2	2.78%	0.23%	96.98%

(**e**) Basic section

Figure 9. Confusion matrix for different segments of LightGBM classification model.

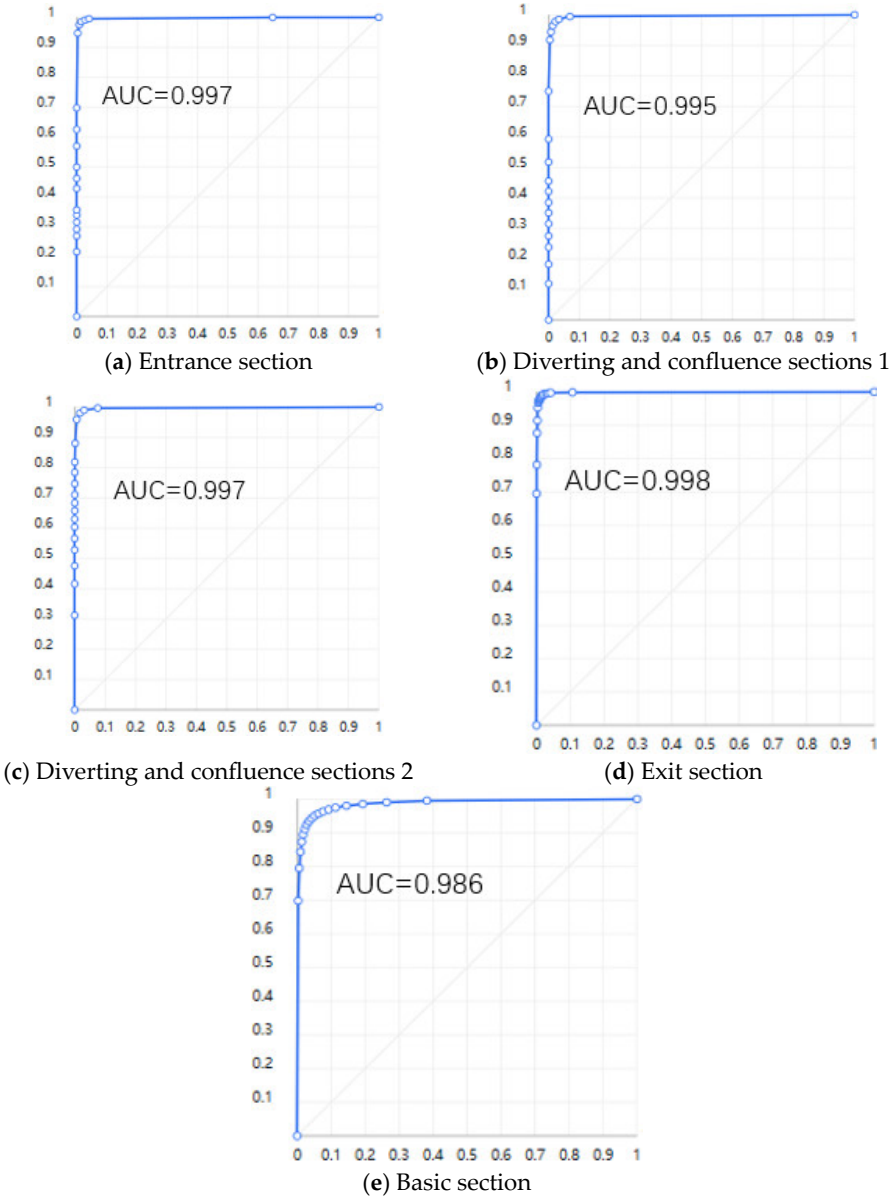

(**a**) Entrance section (**b**) Diverting and confluence sections 1

(**c**) Diverting and confluence sections 2 (**d**) Exit section

(**e**) Basic section

Figure 10. ROC curves for different segments of LightGBM classification model.

For the entrance section's dataset, the length of the deceleration section, the driver's driving time, and the type of deceleration section were the three most important indicators affecting the model. This played a significant role, further verifying the success of optimizing the entrance deceleration markings. Additionally, the driver's driving time ranked second, indicating that over time, the driver's driving safety and comfort changed significantly after entering the tunnel. This demonstrated that the simulation in this study successfully replicated the impact of illumination at the entrance on the driver's natural driving behavior.

For the diverging and merging sections, the top three indicators were acceleration, steering wheel torque, and warning signs. This indicates that, from the perspective of driving behavior, drivers controlled the vehicle's speed more frequently and paid more attention to the information on the notice boards in these sections. Therefore, to improve driving safety and comfort in the diverging and merging sections of underground interchanges, it is essential to optimize the setting of warning signs.

Figure 11. Feature importance ranking diagram of LightGBM model.

There was little difference in the importance of ranking of various factors for the exit section, indicating that these factors collectively played a specific role in classifying the driving safety and comfort evaluation grades of the exit section. This shows that the driving safety and comfort of the exit section results from the joint action of multiple factors, which need to be comprehensively considered for evaluation.

Similarly, for several special sections of the underground interchange, there was little difference in the importance ranking of various factors, indicating that the driving safety and comfort of these special sections were influenced by multiple factors. Therefore, when considering the influencing factors, it is necessary to conduct a careful analysis of multiple aspects to obtain a comprehensive evaluation and better optimization plan. When designing the setting plan for traffic safety facilities, it is essential to develop each special section comprehensively and consider various factors, such as markings and wall colors, to improve driving safety and comfort in the underground interchange.

For the basic segment, acceleration was the only significantly important influencing factor. This result can be attributed to the relatively stable driving conditions in the basic

section, where traffic safety facilities do not have a significant impact as in other special sections. In this case, drivers only need to pay attention to speed changes in the driving direction. Therefore, acceleration has become a crucial indicator in evaluating driving safety and comfort in the basic segment.

Understanding the feature importance rankings provides valuable insights for traffic engineers focused on optimizing safety and comfort in underground interchanges. For example, high-ranking features like entrance signage and deceleration zones indicate that these elements significantly impact driving behavior. Traffic engineers can prioritize these areas for improvements, such as optimizing sign placement and enhancing deceleration markings, to better guide drivers through underground sections. Lower-ranked features, while still relevant, may require less immediate focus, allowing engineers to allocate resources more effectively based on the identified priorities.

4. Conclusions

This study utilized driving simulators and machine learning models to assess the safety and comfort of underground interchanges. Key safety indicators such as speed, acceleration, and accelerator pedal usage, along with comfort indicators like lateral acceleration, acceleration disturbance, and steering wheel torque, were used to build a comprehensive database from 12 multimodal indices obtained through driving simulation tests. The LightGBM model demonstrated strong classification performance, achieving an average accuracy of 97.06%, significantly outperforming other mainstream models. The results also showed that entrance signage and deceleration sections had the greatest impact on driving safety and comfort, while basic road sections were less influential. These findings underscore the importance of optimizing visual cues, including markings and wall colors, in critical areas of underground interchanges. However, the relatively small sample size may limit the generalizability of the results, suggesting the need for further validation with larger datasets in future research.

Author Contributions: Conceptualization, Q.L. and Z.L.; methodology, Z.L.; software, Q.L.; validation, Q.L., C.Z. and B.C.; formal analysis, Q.L. and C.Z.; investigation, B.C. and Z.L.; resources, Z.L.; data curation, Z.L.; writing–original draft preparation, Q.L. and Z.L.; writing–review and editing, B.C., Z.L. and C.Z.; supervision, Z.L.; funding acquisition, Q.L. All authors have read and agreed to the published version of the manuscript.

Funding: This research received no external funding.

Institutional Review Board Statement: Not applicable.

Informed Consent Statement: Not applicable.

Data Availability Statement: The data presented in this study are available on request from the corresponding author.

Conflicts of Interest: The authors declare no conflicts of interest.

References

1. Barati, N.; Zadegan, S.A.H.; Kasravi, R. The role of survey details for wayfinding problem in complex pedestrian underground interchange with poor architectural configuration. *Tunn. Undergr. Space Technol.* **2021**, *108*, 103718. [CrossRef]
2. Liu, Z.; Gu, X.; Hong, R. Fire protection and evacuation analysis in underground interchange tunnels by integrating BIM and numerical simulation. *Fire* **2023**, *6*, 139. [CrossRef]
3. Hong, R.; Liu, Z.; Gu, X. Study on measurement and simulation of noise field between long tunnel and underground interchange. In Proceedings of the Fourth International Conference on Smart City Engineering and Public Transportation (SCEPT 2024), Beijing, China, 26–28 January 2024; SPIE: Bellingham, WA, USA; pp. 28–34.
4. Hong, R.; Liu, Z. Numerical Simulation Research of Fire Behavior and Evacuation in Underground Interchanges. In Proceedings of the 2023 4th International Conference on Computer Science and Management Technology, Xi'an, China, 13–15 October 2023; Association for Computing Machinery: New York, NY, USA; pp. 487–490.
5. Huang, Y.; Chen, F.; Song, M.; Pan, X.; You, K. Effect evaluation of traffic guidance in urban underground road diverging and merging areas: A simulator study. *Accid. Anal. Prev.* **2023**, *186*, 107036. [CrossRef] [PubMed]

6. Wan, L.; Yan, Y.; Zhang, C.; Liu, C.; Mao, T.; Wang, W. Characteristics and identification of risky driving behavior in expressway tunnel based on behavior spectrum. *Int. J. Transp. Sci. Technol.* 2023, *in press*. [CrossRef]
7. Cui, B.; Wang, H. Compatibility analysis of waste polymer recycling in asphalt binder using molecular descriptor and graph neural network. *Resour. Conserv. Recycl.* **2025**, *212*, 107950. [CrossRef]
8. Liu, Z.; Zhou, Z.; Gu, X.; Sun, L.; Wang, C. Laboratory evaluation of the performance of reclaimed asphalt mixed with composite crumb rubber-modified asphalt: Reconciling relatively high content of RAP and virgin asphalt. *Int. J. Pavement Eng.* **2023**, *24*, 2217320. [CrossRef]
9. Sekadakis, M.; Katrakazas, C.; Orfanou, F.; Pavlou, D.; Oikonomou, M.; Yannis, G. Impact of texting and web surfing on driving behavior and safety in rural roads. *Int. J. Transp. Sci. Technol.* **2023**, *12*, 665–682. [CrossRef]
10. Qiao, Y.-K.; Peng, F.-L.; Dong, Y.-H.; Lu, C.-F. Planning an adaptive reuse development of underutilized urban underground infrastructures: A case study of Qingdao, China. *Undergr. Space* **2024**, *14*, 18–33. [CrossRef]
11. Feng, J.R.; Gai, W.-m.; Yan, Y.-b. Emergency evacuation risk assessment and mitigation strategy for a toxic gas leak in an underground space: The case of a subway station in Guangzhou, China. *Saf. Sci.* **2021**, *134*, 105039. [CrossRef]
12. Wang, S.; Du, Z.; Zheng, H.; Han, L.; Xia, X.; He, S. Improving driving safety in freeway tunnels: A field study of linear visual guiding facilities. *Tunn. Undergr. Space Technol.* **2024**, *143*, 105489. [CrossRef]
13. Ma, S.; Yan, X. Examining the efficacy of improved traffic signs and markings at flashing-light-controlled grade crossings based on driving simulation and eye tracking systems. *Transp. Res. Part F Traffic Psychol. Behav.* **2021**, *81*, 173–189. [CrossRef]
14. Fiolić, M.; Babić, D.; Babić, D.; Tomasović, S. Effect of road markings and road signs quality on driving behaviour, driver's gaze patterns and driver's cognitive load at night-time. *Transp. Res. Part F Traffic Psychol. Behav.* **2023**, *99*, 306–318. [CrossRef]
15. Lin, Z.; Chen, F. How various urgencies and visibilities influence drivers' takeover performance in critical car-following conditions? A driving simulation study. *Transp. Res. Part F Traffic Psychol. Behav.* **2024**, *104*, 303–317. [CrossRef]
16. Gao, M.; Zhao, Y.; Shen, Y.; Yu, X.; Gou, S.; Bao, Q. Which factors are most relevant to drivers' overtaking choices at two-lane highways: A comparative analysis between questionnaire surveys and driving simulation. *Transp. Res. Part F Traffic Psychol. Behav.* **2023**, *95*, 202–214. [CrossRef]
17. Horberry, T.; Anderson, J.; Regan, M.A. The possible safety benefits of enhanced road markings: A driving simulator evaluation. *Transp. Res. Part F Traffic Psychol. Behav.* **2006**, *9*, 77–87. [CrossRef]
18. Cui, H.; Yuan, X.; Zhu, M.; Liu, S. The family climate for road safety scale in young Chinese drivers: An analysis of reliability and validity. *Transp. Res. Part F Traffic Psychol. Behav.* **2024**, *103*, 512–525. [CrossRef]
19. Ali, Y.; Raadsen, M.P.H.; Bliemer, M.C.J. Effects of passing rates on driving behaviour in variable speed limit-controlled highways: Evidence of external pressure from a driving simulator study. *Transp. Res. Part F Traffic Psychol. Behav.* **2024**, *104*, 488–505. [CrossRef]
20. Li, Y.; Zhang, X.; Zeng, X.; Qin, K.; Gao, Y. Influence mechanism of the urban traffic climate on prosocial driving behavior: The combined role of rational, affective and moral factors. *Transp. Res. Part F Traffic Psychol. Behav.* **2024**, *104*, 118–135. [CrossRef]
21. Zhang, Z.; Jia, L. Optimal multiobjective design of guidance information systems in underground spaces: Model development and a transportation hub case study. *Tunn. Undergr. Space Technol.* **2023**, *134*, 105007. [CrossRef]
22. Hsu, C.-C.; Chuang, K.-H. Traffic and environmental cues and slow-down behaviors in virtual driving. *Percept. Mot. Ski.* **2016**, *122*, 101–122. [CrossRef]
23. Zhang, C. Net distance between an urban road grade crossing and a tunnel. *J. Highw. Transp. Res. Dev.* **2017**, *11*, 85–89. [CrossRef]
24. Krasniuk, S.; Toxopeus, R.; Knott, M.; McKeown, M.; Crizzle, A.M. The effectiveness of driving simulator training on driving skills and safety in young novice drivers: A systematic review of interventions. *J. Saf. Res.* **2024**, *91*, 20–37. [CrossRef]
25. Pan, Y.A.; Guo, J.; Chen, Y.; Li, S.; Li, W. Incorporating traffic flow model into A deep learning method for traffic state estimation: A hybrid stepwise modeling framework. *J. Adv. Transp.* **2022**, *2022*, 5926663. [CrossRef]
26. Sun, Z.; Xu, J.; Gu, C.; Xin, T.; Zhang, W. Investigation of Car following and Lane Changing Behavior in Diverging Areas of Tunnel–Interchange Connecting Sections Based on Driving Simulation. *Appl. Sci.* **2024**, *14*, 3768. [CrossRef]
27. Liu, Z.; Yang, Q.; Wang, A.; Gu, X. Vehicle Driving Safety of Underground Interchanges Using a Driving Simulator and Data Mining Analysis. *Infrastructures* **2024**, *9*, 28. [CrossRef]
28. Du, Z.; Deng, M.; Lyu, N.; Wang, Y. A review of road safety evaluation methods based on driving behavior. *J. Traffic Transp. Eng.* **2023**, *10*, 743–761. [CrossRef]
29. He, S.; Liang, B.; Pan, G.; Wang, F.; Cui, L. Influence of dynamic highway tunnel lighting environment on driving safety based on eye movement parameters of the driver. *Tunn. Undergr. Space Technol.* **2017**, *67*, 52–60. [CrossRef]
30. Yeung, J.S.; Wong, Y.D. Road traffic accidents in Singapore expressway tunnels. *Tunn. Undergr. Space Technol.* **2013**, *38*, 534–541. [CrossRef]
31. Su, B.; Hu, J.; Zeng, J.; Wang, R. Traffic Safety Improvement via Optimizing Light Environment in Highway Tunnels. *Int. J. Environ. Res. Public Health* **2022**, *19*, 8517. [CrossRef]
32. Liu, Y.; Peng, L.; Lin, L.; Chen, Z.; Weng, J.; Zhang, Q. The impact of LED spectrum and correlated color temperature on driving safety in long tunnel lighting. *Tunn. Undergr. Space Technol.* **2021**, *112*, 103867. [CrossRef]
33. Szydłowski, T.; Surmiński, K.; Batory, D. Drivers' Psychomotor Reaction Times Tested with a Test Station Method. *Appl. Sci.* **2021**, *11*, 2431. [CrossRef]

34. Liu, Q.; Cui, B.; Liu, Z. Air Quality Class Prediction Using Machine Learning Methods Based on Monitoring Data and Secondary Modeling. *Atmosphere* **2024**, *15*, 553. [CrossRef]
35. Pan, Y.A.; Guo, J.; Chen, Y.; Cheng, Q.; Li, W.; Liu, Y. A fundamental diagram based hybrid framework for traffic flow estimation and prediction by combining a Markovian model with deep learning. *Expert Syst. Appl.* **2024**, *238*, 122219. [CrossRef]
36. Wei, Z.; Hou, K.; Jia, Y.; Wang, S.; Li, Y.; Chen, Z.; Zhou, Z.; Gao, Y. Impact of aggregate gradation and asphalt-aggregate ratio on pavement performance during construction using back propagation neural network. *Autom. Constr.* **2024**, *165*, 105569. [CrossRef]
37. Chen, Z.; Jia, Y.; Wang, S.; Wei, Z.; Gao, Y.; Huang, X.; Zhang, Z.; Yan, L. Image-based methods for automatic identification of elongated and flat aggregate particles. *Constr. Build. Mater.* **2023**, *382*, 131187. [CrossRef]
38. Wang, D.; Liu, Z.; Gu, X.; Wu, W. Feature extraction and segmentation of pavement distress using an improved hybrid task cascade network. *Int. J. Pavement Eng.* **2023**, *24*, 2266098. [CrossRef]
39. Chen, Y.; Gu, X.; Liu, Z.; Liang, J. A fast inference vision transformer for automatic pavement image classification and its visual interpretation method. *Remote Sens.* **2022**, *14*, 1877. [CrossRef]
40. Liu, Z.; Wang, S.; Gu, X.; Wang, D.; Dong, Q.; Cui, B. Intelligent Assessment of Pavement Structural Conditions: A Novel FeMViT Classification Network for GPR Images. *IEEE Trans. Intell. Transp. Syst.* **2024**, *25*, 13511–13523. [CrossRef]
41. Tao, P.; Shen, H.; Zhang, Y.; Ren, P.; Zhao, J.; Jia, Y. Status Forecast and Fault Classification of Smart Meters Using LightGBM Algorithm Improved by Random Forest. *Wirel. Commun. Mob. Comput.* **2022**, *2022*, 3846637. [CrossRef]